

Critical behavior of the frustrated antiferromagnetic six-state clock model on a triangular lattice

J. D. Noh and H. Rieger

Theoretische Physik, Universität des Saarlandes, 66041 Saarbrücken, Germany

M. Enderle and K. Knorr

Technische Physik, Universität des Saarlandes, 66041 Saarbrücken, Germany

(Received 3 April 2002; published 20 August 2002)

We study the antiferromagnetic six-state clock model with nearest neighbor interactions on a triangular lattice with extensive Monte Carlo simulations. We find clear indications of two phase transitions at two different temperatures: Below T_I a chirality order sets in and by a thorough finite-size-scaling analysis of the specific heat and the chirality correlation length we show that this transition is in the Ising universality class (with a nonvanishing chirality order parameter below T_I). At T_{KT} ($< T_I$) the spin-spin correlation length as well as the spin susceptibility diverges according to a Kosterlitz-Thouless (KT) form and spin correlations decay algebraically below T_{KT} . We compare our results to recent x-ray diffraction experiments on the orientational ordering of CF_3Br monolayers physisorbed on graphite. We argue that the six-state clock model describes the universal feature of the phase transition in the experimental system and that the orientational ordering belongs to the KT universality class.

DOI: 10.1103/PhysRevE.66.026111

PACS number(s): 05.90.+m, 64.60.Cn, 75.10.Hk, 75.40.Mg

I. INTRODUCTION

The study of frustrated two-dimensional spin models is motivated by their relevance for phase transitions in a wide range of physical systems. For instance, the fully frustrated XY (FFXY) model describes an array of Josephson junctions under an external magnetic field [1,2]. Besides its experimental relevance the FFX model has been the focus of a number of theoretical works since a delicate question arises here regarding the critical behavior. The model has a continuous $U(1)$ symmetry and a discrete Ising, chiral or Z_2 symmetry that can be broken at low temperatures through a Kosterlitz-Thouless (KT)-type transition and an Ising-like transition, respectively.

Despite a lot of effort [3–22], there is no consensus on the nature of the phase transitions and it is not clear whether the two transitions happen at two different temperatures or at a single one. Renormalization group (RG) studies on the FFX model drew the conclusion that the transitions occur at the same temperature [3]. Monte Carlo simulation studies on generalized FFX models supported the single-transition picture for the FFX model [4]. Interestingly, it has been reported that the Z_2 symmetry breaking transition may not belong to the Ising universality class. Monte Carlo studies of the FFX models on a triangular and a square lattice yielded the correlation length exponent $\nu=0.83(4)$ (triangular lattice) and $\nu=0.85(3)$ (square lattice), which is inconsistent with the Ising value $\nu=1$ [5]. The specific heat appeared to follow a power-law scaling rather than the logarithmic scaling as one would expect for the Ising universality class. A non-Ising scaling behavior is also observed in the studies of the FFX model via a Monte Carlo simulation [6] and Monte Carlo transfer matrix calculations [7,8]. The same non-Ising critical behavior is also observed in the coupled XY Ising model [5,9,10].

On the other hand, numerical evidence also in favor of two transitions at two different temperatures has been col-

lected. Monte Carlo simulation studies of the frustrated Coulomb gas system, which is supposed to be in the same universality class as the FFX model, showed that the KT-type transition temperature T_{KT} and the Ising-like transition temperature T_I are different with $T_{KT} < T_I$ [11,12]. Two transitions were also found in the FFX model on a square lattice [13] and on a triangular lattice [14–16] using Monte Carlo simulations. A careful analysis of the RG flow of the FFX model also led to a conclusion of the double transition scenario [17]. It is the general belief that the transitions at T_{KT} and at T_I belong to the KT universality class [18] and to the Ising universality class, respectively, if the transitions occur at different temperatures. However, the critical exponents associated with the Z_2 symmetry breaking, which are found by Monte Carlo simulations, turn out to be different from those of the Ising universality [12,13,16]. They are rather close to those obtained in the XY Ising model [5]. Although there is an argument that the observed non-Ising exponents are due to a screening effect hindering the asymptotic scaling behavior [19], the controversy on the nature of the phase transition remains unsettled [20–22].

Here we present a thorough numerical study of a related model, the fully frustrated antiferromagnetic six-state clock model on a triangular lattice. We also report on an orientational ordering transition in a two-dimensional experimental system [23] that, as we argue, is in the same universality class as the model we study numerically. The experimental system actually motivates (besides numerical simplicity) our restriction to the six states of the spins rather than the continuum XY spins [and thus to a sixfold clock (C_6) symmetry rather than the $U(1)$ symmetry]. In the unfrustrated (ferromagnetic) case it has been shown, however, that the KT behavior is stable with respect to a crystal field of sixfold symmetry [24–26]. Hence we expect that our model displays the same critical behavior as the FFX model.

The paper is organized as follows: In Sec. II we define the model and identify symmetry in the ground state. The corre-

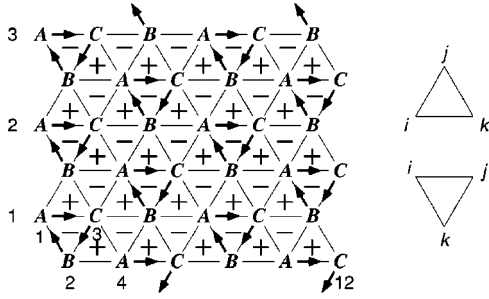


FIG. 1. A triangular lattice of size 12×3 . The arrows represent the spin state in one of the ground states, \mathcal{C}_0 . The lattice sites are labeled by the sublattice indices A , B , and C . Also shown are elementary up and down triangles denoted by Δ_i and ∇_i , respectively. The \pm signs denote the chirality of the triangles.

sponding order parameters are also defined. In Sec. III we explain briefly the Monte Carlo procedure we used and determine the transition temperatures for the two phase transitions. Section IV is devoted to the classification of the universal properties at the two transitions we find. In Sec. V we present experimental x-ray diffraction results on the orientational ordering of CF_3Br monolayers physisorbed on graphite, which we expect to be described by the KT transition occurring in the model we studied numerically in the preceding sections. Section VI concludes the paper with a summary of our results.

II. MODEL

We investigate the phase transitions of the antiferromagnetic six-state clock model on a two-dimensional (2D) $N = L_x \times L_y$ triangular lattice (see Fig. 1). The six-state clock spin \mathbf{S} is a planar spin pointing toward discrete six directions; $\mathbf{S} = (\cos \theta, \sin \theta)$ with

$$\theta = \frac{2\pi n}{6} \quad (n=0,1,\dots,5). \quad (1)$$

The interaction is given by the Hamiltonian

$$\mathcal{H} = 2J \sum_{\langle i,j \rangle} \cos(\theta_i - \theta_j), \quad (2)$$

where the sum is over all nearest neighbor site pairs $\langle i,j \rangle$ and $J > 0$ is the antiferromagnetic coupling strength. The overall factor 2 is introduced for a computational convenience.

The antiferromagnetic interaction on a triangular lattice induces a frustration. As a result the spins on each triangle should make an angle of $\pm 120^\circ$ with one another in the ground state. There are 12-fold degenerate ground states with three-sublattice structure. According to their chirality, we can categorize the ground states into \mathcal{C}_n and \mathcal{A}_n ($n=0,1,\dots,5$). In each ground state the spin configurations of the three sublattices A , B , C (Fig. 1) are given by

$$\theta_{i \in A} = \frac{2\pi n}{6}, \quad \theta_{i \in B} = \frac{2\pi(n \pm 2)}{6}, \quad \theta_{i \in C} = \frac{2\pi(n \pm 4)}{6}, \quad (3)$$

for \mathcal{C}_n (upper sign) and \mathcal{A}_n (bottom sign). In other words, in the $\mathcal{C}(\mathcal{A})$ -type ground state, the spin angles increase by $2\pi/3$ along the up triangles in the (counter) clockwise direction, and vice versa for down triangles.

There are two different symmetries between them; those in the same class of \mathcal{C} or \mathcal{A} are related by the rotation $\theta_i \rightarrow \theta_i + (2\pi m/6)$ ($m=0, \dots, 5$) and those in the others by the reflection $\theta_i \rightarrow -\theta_i$. Therefore the model possesses the C_6 (six-fold clock) symmetry and the Z_2 (Ising) symmetry. Note that the FFXY model on a triangular lattice has a $U(1)$ and a Z_2 symmetry [2]. Since the clock spin can have only six states, while the XY spin is a continuous one, the continuous $U(1)$ symmetry of the FFXY model is reduced to the discrete C_6 symmetry. The nature of the Z_2 symmetry in each model is identical.

From the symmetry consideration, we expect that there are two types of phase transitions associated with the spontaneous breaking of the C_6 symmetry and the Z_2 symmetry. The chirality at each elementary triangle is defined as

$$h_{\Delta_i, \nabla_i} = \frac{2}{3\sqrt{3}} [\sin(\theta_j - \theta_i) + \sin(\theta_k - \theta_j) + \sin(\theta_i - \theta_k)],$$

where Δ_i and ∇_i are up and down triangles as depicted in Fig. 1. Then the ground state $\mathcal{C}_n(\mathcal{A}_n)$ has a checkerboard pattern of the chirality with $h_{\Delta} = +1$ (-1) and $h_{\nabla} = -1$ ($+1$). The staggered chirality

$$h = \frac{1}{2N} \sum_i (h_{\Delta_i} - h_{\nabla_i}) \quad (4)$$

plays a role of the order parameter for the Z_2 symmetry breaking transition. The order parameter for the C_6 symmetry breaking transition is the sublattice magnetization

$$m_A = \frac{1}{N} \sum_{i \in A} \exp(i\theta_i), \quad (5)$$

where the sum runs only over the sites in the A sublattice. m_B and m_C are defined analogously.

III. TRANSITION TEMPERATURES

We performed Monte Carlo (MC) simulations on finite $N = L \times (L/2)$ lattices with a sublattice updating scheme; one of the three sublattices is selected randomly and then all spins in the chosen sublattice are flipped according to the Metropolis rule. One Monte Carlo step corresponds to three sublattice updates. Various observables are measured during the MC runs, such as the energy, the chirality, and the sublattice magnetization, from which we can measure the averaged quantities and their fluctuations. In some cases, histograms are constructed from particularly long MC runs to obtain the observables as continuous functions of the temperature.

The transition temperature is determined from the Binder parameters

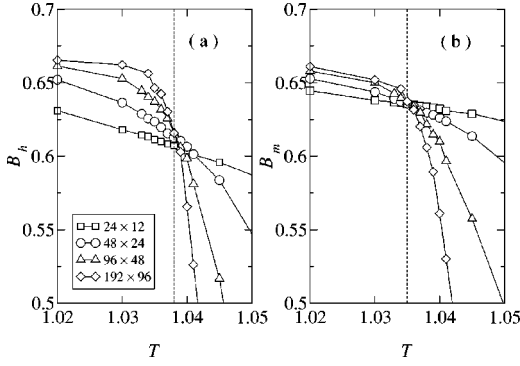


FIG. 2. Binder parameters for the staggered chirality in (a) and the magnetization in (b). The estimated transition temperatures are marked by broken lines.

$$B_h = 1 - \frac{\langle h^4 \rangle}{3\langle h^2 \rangle^2} \quad \text{and} \quad B_m = 1 - \frac{\langle m_A^4 \rangle}{3\langle m_A^2 \rangle^2} \quad (6)$$

for the chirality and the magnetization, respectively. Here the angle bracket denotes a thermal average, which can be done by a time average over the MC runs. The Binder parameters are scale independent at the critical points and approaches $\frac{2}{3}$ (0) in the ordered (disordered) phase as L becomes larger. Hence the order-disorder transition temperature T_I related to the Z_2 symmetry breaking is obtained from the crossing point in the plot of B_h versus T at different system sizes. From Fig. 2(a), we estimate that

$$T_I = 1.038 \pm 0.0005. \quad (7)$$

B_m also displays the crossing behavior [Fig. 2(b)], from which we estimate that

$$T_{KT} = 1.035 \pm 0.0005 \quad (8)$$

for the C_6 symmetry breaking transition.

The Binder parameters show different size dependence at low temperatures. For the staggered chirality B_h converges rapidly to $2/3$ as L increases. However, B_m appears to converge to values less than $2/3$ at $T < T_{KT}$. It indicates that there is a quasi-long-range order in spins at $T < T_{KT}$. We confirm it from finite-size-scaling (FSS) behaviors of the magnetization. The sublattice magnetization shows the power-law scaling behavior, $\langle |m_A| \rangle \sim L^{-x}$, at $T \leq T_{KT}$ with temperature dependent exponent x (see Fig. 3).

The two transition temperatures lie very close to each other. Nevertheless the accuracy of the data is sufficiently high, so that we can exclude a possibility $T_I = T_{KT}$. Figure 4 demonstrates this via the correlation functions. We measure the correlations between the chirality of up triangles and the magnetization of spins in the A sublattice displaced by a distance r in the vertical direction:

$$C_h(r) = \left\langle \frac{3}{N} \sum_{i \in A} h_{\Delta_i} h_{\Delta_{i+r}} \right\rangle, \quad (9)$$

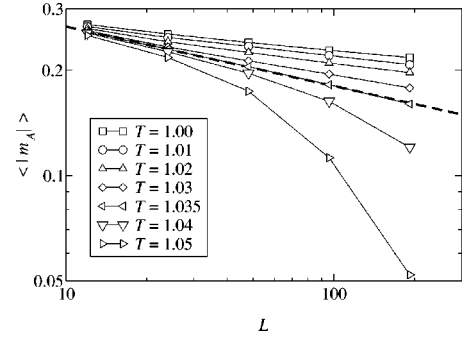


FIG. 3. Sublattice magnetization $\langle |m_A| \rangle$ near the critical temperature T_{KT} . At temperatures $T \leq T_{KT}$ it shows a power-law behavior. The broken line has a slope of -0.17 .

$$C_m(r) = \left\langle \frac{3}{N} \sum_{i \in A} \cos(\theta_i - \theta_{i+r}) \right\rangle. \quad (10)$$

Here, $i+r$ denotes a site displaced vertically by a distance r from i , and Δ_i denotes an up triangle whose left corner is i (see Fig. 1). In Fig. 4, we plot both correlation functions in the log-log scale at an intermediate temperature $T = 1.037$. Clearly one can see an upward curvature in the plot of $C_h(r)$ for $r \ll L_y/2$, which implies that the chirality order has already set in. On the other hand, there is a downward curvature in the plot of $C_m(r)$ for $r \ll L_y/2$ indicating that the magnetic order has not set in yet. Therefore we conclude that $T_{KT} < 1.037 < T_I$.

IV. UNIVERSALITY CLASS

With $T_{KT} \neq T_I$, one expects that both the symmetry breakings take place independently. Then, the Z_2 symmetry breaking transition should be in the Ising universality class. The C_6 symmetry is equivalent to that of the XY model perturbed by the ($p=6$)-fold anisotropy field. The unperturbed XY model displays a KT transition that separates a disordered high-temperature phase and a quasi-long-range ordered low-temperature phase. A RG study shows that an anisotropy field with $p > 4$ does not change the KT nature of the transition [24]. The same is true for the extreme case of the ferromagnetic six-state clock model [26]. So the C_6 symmetry

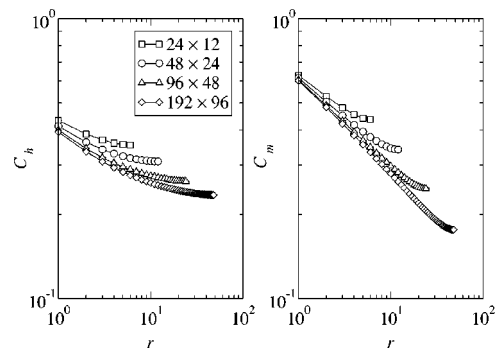


FIG. 4. Correlation functions of the staggered chirality, C_h , and the magnetization, C_m , at temperature $T = 1.037$.

breaking phase transition at $T=T_{KT}$ is expected to belong to the KT universality class.

The interplay of the Ising-type and the KT-type ordering has long been studied in the context of the fully frustrated XY models on a square or a triangular lattice. Frequently, it has been claimed [3–8] that the Ising-like transition and the KT-type transition occur at the same temperature. On the other hand, more recent studies have reported the transitions to occur at two different temperatures [11–17,19,20,22]. Surprisingly, some of recent high-precision Monte Carlo simulation studies suggested that the Z_2 symmetry breaking transition does not belong to the Ising universality class in spite of the double transition [13,16,22]. They estimated that $\nu \approx 0.8$ for the correlation length exponent and $\alpha/\nu \approx 0.46$ with the specific exponent α , which are incompatible with the Ising values of $\nu=1$ and $\alpha=0$. The critical exponents are consistent with the values observed along the single transition line of the coupled XY Ising model [5,9,10]. Olsson [19] argued that the measured non-Ising critical exponents are artifacts of unusual finite-size effects originated from non-critical spin-wave fluctuations. However, apparently there is no general agreement yet on this subject [20].

In our model, we observe the phase transitions occurring at two *different* temperatures. However, the controversy existing in the FFXY model tells us that it does not guarantee necessarily that the individual transitions will belong to the KT universality class and the Ising universality class, respectively. Therefore we perform a thorough FSS analysis to understand the nature of the phase transition. We believe that the antiferromagnetic six-state clock model can be used to resolve the existing controversy for the FFXY model. It has the proper symmetry properties as discussed previously. And, from a practical point of view, larger system sizes are available since it is a discrete model, with which one can reduce the finite-size effects.

A. Z_2 symmetry breaking

We investigate the nature of the Z_2 symmetry breaking transition by exploring the FSS property of the specific heat, which is defined by

$$c = N[\langle e^2 \rangle - \langle e \rangle^2], \quad (11)$$

with e the energy per site. For a finite system [$N=L(L/2)$] the specific heat has a peak $c_* \sim L^{\alpha/\nu}$ near the critical temperature, diverging with system size $L \rightarrow \infty$. Since the specific heat does not diverge at a KT-type transition, the divergence is due to the Z_2 symmetry breaking phase transition. The Ising universality class has $\alpha=0$, and the specific heat shows a logarithmic divergence, $c_* \sim \ln L$.

The specific heat is measured accurately using the standard MC method combined with a *single histogram method* [27]. First, we measure the specific heat from the standard MC simulations at discrete temperature grid, which leads to a temperature T_0 at which the specific heat is approximately maximum. Then the histogram $\Omega_0(\{\mathbf{S}\})$, frequency of a spin state $\{\mathbf{S}\}$, is constructed from MC runs at the temperature T_0

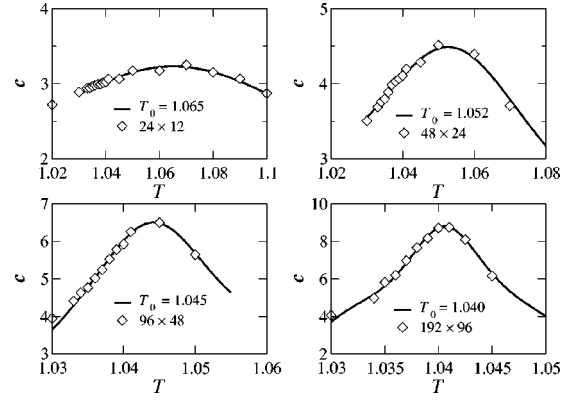


FIG. 5. Specific heat obtained from independent MC runs (symbols) and the histogram method (solid lines). T_0 denotes the temperature at which the histogram is obtained.

over a time interval Δt . It enables us to obtain the average value of any observable Q as a continuous function of temperature T near T_0 ;

$$\langle Q \rangle = \frac{\sum_{\{\mathbf{S}\}} Q(\{\mathbf{S}\}) \Omega_0(\{\mathbf{S}\}) e^{-(T^{-1}-T_0^{-1})E(\{\mathbf{S}\})}}{\sum_{\{\mathbf{S}\}} \Omega_0(\{\mathbf{S}\}) e^{-(T^{-1}-T_0^{-1})E(\{\mathbf{S}\})}}. \quad (12)$$

It is important to take Δt as large as possible to have good statistics. At 192×96 lattice, for example, we take $\Delta t = 5 \times 10^7$, which is ~ 2000 times the relaxation time of energy-energy autocorrelation. The maximum system size we can simulate is 384×192 . In that case we take $\Delta t = 10^8$, which is ~ 1200 times the relaxation time of energy-energy autocorrelation. Figure 5 shows the specific heat obtained from independent MC runs and from the histogram method. Their agreement near the peak is excellent, although they begin to deviate slightly away from the peak. With this technique we can estimate c_* very accurately. A statistical error for c_* is estimated in the following way; we construct ten subhistograms and as many values of c_* from each of them. The error bar is taken as the half distance between the maximum and minimum values among them.

The result is shown in Fig. 6. Interestingly, there is a crossover from a power-law scaling behavior $c_* \sim L^{0.5}$ [solid

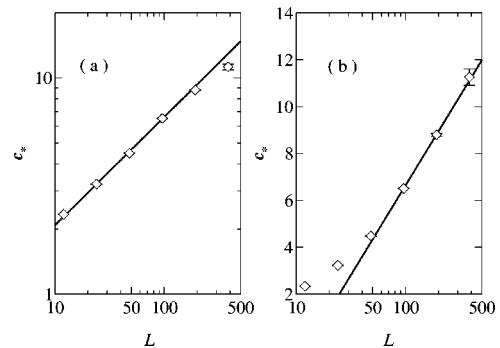


FIG. 6. Peak values of the specific heat versus L in log-log scale (a) and semilog scale (b). In (a) the solid line has a slope 0.5.

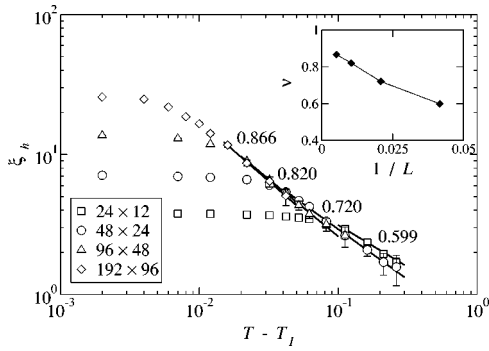


FIG. 7. Chirality correlation length. The values of the exponent ν obtained from the fit at each lattice size are shown in the main panel and plotted in the inset.

line in Fig. 6(a) at $L \leq L_c$ to a logarithmic scaling behavior $c_* \sim \ln L$ [solid line in Fig. 6(b)] at $L \geq L_c$ with $L_c \approx 96$. It indicates that the specific heat has an asymptotical logarithmic scaling behavior that is consistent with the Ising universality class.

We also study the scaling of the chirality correlation length. We measured the correlation length using $\xi_h = \sqrt{\sum_r r^2 C_h(r) / \sum_r C_h(r)}$ with the correlation function defined in Eq. (9). It is plotted in Fig. 7. We find a strong dependence of ξ_h on the system size. In addition to the saturation of ξ_h to $O(L)$ near and below the critical point, the dependence of the correlation length on L in the regime $\xi_h \ll L$ is visible through a varying slope (cf., Fig. 7). As a consequence, a fitting to a form $\xi_h = a(T - T_I)^{-\nu}$ at small system size will lead to a lower value of ν than its asymptotic value. The fitted values of ν at each lattice size are plotted in the inset of Fig. 7. It increases as the system size increases and approaches the Ising value $\nu \approx 1.0$ in the infinite size limit.

From the analysis of the specific heat and the chirality correlation length, we conclude that the Z_2 symmetry breaking transition indeed belongs to the Ising universality class. Note that the *effective* specific heat exponent $\alpha/\nu \approx 0.5$ and the correlation length exponent $\nu \approx 0.8$ appearing at small length scale are comparable with the results of previous MC works claiming the non-Ising nature in the frustrated XY models [5,6,9,10,13,16,21,22]. Our results are fully consistent with Olsson's argument claiming that the non-Ising exponents reported by others are explained by a failure of finite-size scaling at small length scale due to the screening length associated with the nearby KT transition [19]. The strong finite-size effect is overcome in this work since we could study large systems. We expect that one could observe the same crossover to the asymptotic Ising-type scaling behavior in larger scale simulations in the frustrated XY systems.

B. C_6 symmetry breaking

The KT transition is characterized by the essential singularity of the correlation length and the susceptibility approaching the critical temperature. We measure the correlation length ξ_m as

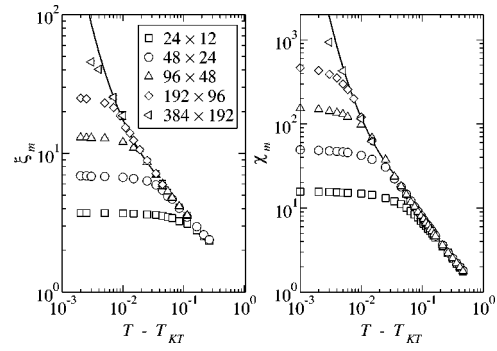


FIG. 8. Correlation length and the susceptibility of the magnetization. The solid lines are the fits to the KT form of $\xi_m = 2.54e^{0.193(T - T_{KT})^{-1/2}}$ and $\chi_m = 4.20e^{0.333(T - T_{KT})^{-1/2}}$.

$$\xi_m = \sqrt{\frac{\sum_r r^2 C_m(r)}{\sum_r C_m(r)}} \quad (13)$$

from the magnetic correlation function C_m in Eq. (10). One can also estimate the correlation length by fitting $C_m(r)$ to a form with e^{-r/ξ_m} . We tried with various function forms but found that Eq. (13) yields the most stable estimate against statistical errors. The magnetic susceptibility is measured from the fluctuation of the magnetization, $\chi_m = N \langle m_A^2 \rangle$. Figure 8 shows the plot of ξ_m and χ_m versus $T - T_{KT}$ in log-log scale. Upward curvature in both plots indicates a divergence stronger than algebraic. We fit those quantities with the KT scaling form, $\xi_m = a e^{b(T - T_{KT})^{-y}}$ and $\chi_m = a' e^{b'(T - T_{KT})^{-y}}$ with $y = \frac{1}{2}$ fixed, whose results are drawn with solid lines in Fig. 8. It shows that the KT scaling behaviors are emerging only after $L \geq 96$. If y is also taken as a fitting parameter, one obtains $y < 0.5$ whose value depends on the fitting range; it increases on approaching the critical temperature.

In the XY phase ($T < T_{KT}$) the spins have the quasi-long-range order; the magnetization scales algebraically as $\langle |m_A| \rangle \sim L^{-x}$ with temperature dependent exponent x (see Fig. 3). The RG theory predicts that $x = 1/8$ at the KT transition point [24]. Our numerical data show that $x \approx 0.17$ at $T = T_{KT}$. We think that the discrepancy is originated from a sensitive dependence of x on T . In summary, in spite of a quantitative disagreement, the C_6 symmetry breaking phase transition is in qualitative agreement with the KT universality class; we observe the essential singularity in the correlation length and the susceptibility and quasi-long-range order in the low-temperature phase.

V. EXPERIMENTAL REALIZATION: CF₃Br ON GRAPHITE

In this section we describe a possible experimental realization of the theoretical model we investigated above. In a recent work we reported results on x-ray powder diffraction study on a monolayer of halomethane CF₃Br adsorbed on exfoliated graphite [23]. CF₃Br is a prolate molecule and has a dipole moment of about 0.5 D. The coverage ρ and the

temperature T phase diagram is rather complex [28,29]. In Ref. [23] we concentrated on a coverage that is a representative of the extended monolayer regime in which the monolayer lattice is commensurate with the graphite lattice. This yields a 2×2 triangular lattice arrangement of the CF_3Br molecules below a temperature of 105 K [30], which is the melting temperature of the commensurate layer. The intermolecular distance is $a = 4.92 \text{ \AA}$. Note that the lateral size of the graphite crystallites is only around 180 \AA , which confines any spatial correlation length to this value.

An isolated CF_3Br would prefer to lie flat on the substrate, but the 2×2 mesh is too tight to accommodate the molecules in this orientation. Therefore the individual CF_3Br molecules stand on the substrate, presumably with the F_3 tripod down, with a maximum tilt angle of the molecular axis up to 30° with respect to the substrate normal due to steric repulsion. A tilt leads to a nonzero in-plane component of the dipole moment. We regard this component as planar pseudospin $\mathbf{S}_i = (\cos \theta_i, \sin \theta_i)$ with the azimuthal angle θ_i of the molecule. In this sense the 2×2 state is disordered with a zero time average of every \mathbf{S}_i , and is stabilized at higher temperatures by a libration and/or a precession of the molecular axis about the substrate normal.

As the temperature is decreased additional features develop in the diffraction pattern that finally, below 40 K, can be identified [23] as Bragg peaks (with a finite width of around $(180 \text{ \AA})^{-1}$ due to the lateral size of the crystallites) indicating an orientational order in the dipole moments identical to the one depicted in Fig. 1. The temperature dependence of the correlation length ξ determined from the intrinsic width of this peak can be fitted, with the KT expression

$$\xi = A \exp[B(T/T_{KT} - 1)^{-1/2}], \quad (14)$$

to the data for $T > 40 \text{ K}$ (see Fig. 3 of Ref. [23]). The fit parameters are $A = 9 \pm 2 \text{ \AA}$, $B = 1.5 \pm 0.4$, and $T_{KT} = 30 \pm 3 \text{ K}$. Note that the value of A is reasonably close to the lattice parameter of the 2D mesh. Thus ξ is expected to diverge at a KT critical temperature T_{KT} of about 30 K, but the growth of the correlated regions is interrupted when ξ reaches the size of the graphite crystallites. This happens at about 40 K.

We think that the model (2) is a good description of the orientational ordering process described in this physical system. Clearly the pseudospin correlations are bound to a plane, thus the system is 2D with respect to the relevant degrees of freedom at the phase transition. Moreover, as mentioned before, below 105 K the CF_3Br molecules are arranged in a triangular lattice. The pseudospin representing the CF_3Br dipole moment is presumably not a strictly isotropic planar rotator but experiences a crystal field from the graphite substrate, which breaks the continuous azimuthal symmetry into the sixfold symmetry of the monolayer. This is reflected by the six-state clock variables of model (2). The ordered structure of the CF_3Br dipoles is antiferroelectric, which is taken into account by the antiferromagnetic couplings between the pseudospins in Eq. (2). Finally, the character of the relevant orientation dependent interactions of CF_3Br is not known, but a comparison of monolayers of

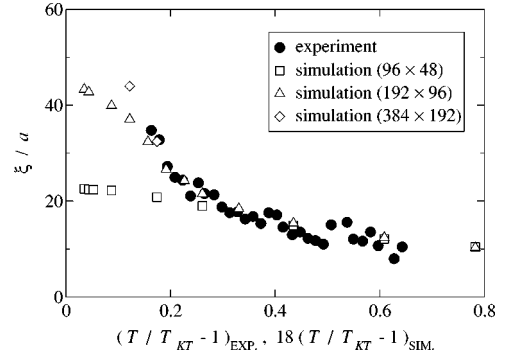


FIG. 9. Comparison of the magnetic correlation length (scaled by the lattice constant) from the experimental data (from Fig. 3 of Ref. [23]) and the Monte Carlo simulations (from Fig. 8). The reduced temperatures $(T/T_{KT} - 1)$ for the simulation data are rescaled by a factor of 18 in order to achieve an acceptable data collapse for linear lattice sizes L between 96 and 192.

several polar methane derivatives [29] shows that fully halogenated molecules including CF_3Br with small dipole moments around 0.5 D have structures different from partially halogenated molecules, such as CH_3Cl , with strong dipole moments around 1.7 D. This suggests that for CF_3Br the short-range anisotropic part of the intermolecular van der Waals force and hardcore repulsion are more important than the medium-range dipole-dipole interaction. Thus the interactions can be assumed to be short ranged. Thus one expects that model (2) and the physical system discussed here are in the same universality class.

In Fig. 9(a) comparison of the magnetic correlation length from the experiment [23] and the simulation (from Fig. 8) is shown. Since the factor B in the KT form (14) of the correlation length is a nonuniversal number, the reduced temperature $(T/T_{KT} - 1)$ has to be rescaled by an appropriate factor in order to achieve an acceptable data collapse. The rescaling factor turns out to be quite large, namely 18, which is not unusual for microscopically different systems in the KT universality class (see, e.g., Ref. [31]). Note that the finite linear size of the crystallites plays a similar role as the finite lattice sizes in the simulations and sets the saturation value for the correlation length (divided by the lattice constant for the triangular lattice of the CF_3Br molecules, which is $a = 4.92 \text{ \AA}$). The nice collapse of the experiment and simulation data supports our claim that the two physical systems are in the same universality class and that the orientational ordering of CF_3Br molecules on graphite is in the KT universality class.

VI. SUMMARY

To summarize we have studied the phase transitions in the antiferromagnetic six-state clock model on a triangular lattice, which is fully frustrated. As a result the ground states have a C_6 (six-state clock) symmetry and a Z_2 (Ising) symmetry. Through extensive Monte Carlo simulations we found that the model undergoes a Kosterlitz-Thouless transition at T_{KT} and an Ising transition at T_I . The two transitions corre-

spond to the C_6 and the Z_2 symmetry breaking transition, respectively. High-precision Monte Carlo data indicate that the two transitions take place at different temperatures, $T_{KT} < T_I$ [Eqs. (7) and (8)]. This has been checked explicitly by analyzing the behavior of the spin and the chirality correlation function at temperatures between T_{KT} and T_I (Fig. 4). Furthermore, we have shown that the Z_2 symmetry breaking transition belongs to the Ising universality class. For small system sizes, the scaling property of the specific heat and the correlation length deviates apparently from the Ising universality class. However, simulation results for larger system sizes indicate that the model belongs asymptotically to the Ising universality class (Figs. 6 and 7). As for the transition at T_{KT} , we have found that the magnetization correlation length and the susceptibility diverges at $T = T_{KT}$ according to the KT scaling form (Fig. 8). We have also found that the spins have a quasi-long-range order below T_{KT} (Fig. 3). Combining these, we conclude that the transition at T_{KT} belongs to the KT universality class.

Our model is a variant of the fully frustrated XY models where the KT-type ordering and the Ising-type ordering interplay interestingly. Our numerical results support a sce-

nario that there are two separate phase transitions with $T_{KT} \neq T_I$; one at T_{KT} in the KT universality class and the other at T_I in the Ising universality class. Our results are very well consistent with those in Ref. [19].

We have proposed that our theoretical model describes the orientational ordering transition of CF_3Br molecules on graphite since the model has the same symmetry as the experimental system. We argue that the orientational ordering transition belongs to the KT universality class [23] by comparing the magnetic correlation length obtained from the experiment [23] with the correlation length obtained numerically in the six-state clock model. With a suitable rescaling of parameters, we have shown that the correlation lengths in both systems have the same scaling behavior (Fig. 9). It gives more evidence that the orientational ordering transition is indeed the KT transition.

ACKNOWLEDGMENT

This work has been supported by the Deutsche Forschungsgemeinschaft (DFG).

-
- [1] S. Teitel and C. Jayaprakash, Phys. Rev. B **27**, 598 (1983).
 - [2] D.H. Lee, J.D. Joannopoulos, J.W. Negele, and D.P. Landau, Phys. Rev. Lett. **52**, 433 (1984); Phys. Rev. B **33**, 450 (1986).
 - [3] M.Y. Choi and D. Stroud, Phys. Rev. B **32**, 5773 (1985); M. Yosefin and E. Domany, Phys. Rev. B **32**, 1778 (1985).
 - [4] B. Berge, H.T. Diep, A. Ghazali, and P. Lallemand, Phys. Rev. B **34**, 3177 (1986); H. Eikmans, J.E. van Himbergen, H.J.F. Knops, and J.M. Thijssen, Phys. Rev. B **39**, 11 759 (1989).
 - [5] J. Lee, J.M. Kosterlitz, and E. Granato, Phys. Rev. B **43**, 11 531 (1991).
 - [6] G. Ramirez-Santiago and J.V. José, Phys. Rev. Lett. **68**, 1224 (1992); Phys. Rev. B **49**, 9567 (1994).
 - [7] E. Granato and M.P. Nightingale, Phys. Rev. B **48**, 7438 (1993).
 - [8] Y.M.M. Knops, B. Nienhuis, H.J.F. Knops, and H.W.J. Blöte, Phys. Rev. B **50**, 1061 (1994).
 - [9] E. Granato, J.M. Kosterlitz, J. Lee, and M.P. Nightingale, Phys. Rev. Lett. **66**, 1090 (1991).
 - [10] M.P. Nightingale, E. Granato, and J.M. Kosterlitz, Phys. Rev. B **52**, 7402 (1995).
 - [11] G.S. Grest, Phys. Rev. B **39**, 9267 (1989).
 - [12] J.-R. Lee, Phys. Rev. B **49**, 3317 (1994).
 - [13] S. Lee and K.-C. Lee, Phys. Rev. B **49**, 15 184 (1994).
 - [14] S. Miyashita and H. Shiba, J. Phys. Soc. Jpn. **53**, 1145 (1984).
 - [15] H.-J. Xu and B.W. Southern, J. Phys. A **29**, L133 (1996).
 - [16] S. Lee and K.-C. Lee, Phys. Rev. B **57**, 8472 (1998).
 - [17] G.S. Jeon, S.Y. Park, and M.Y. Choi, Phys. Rev. B **55**, 14 088 (1997).
 - [18] J.M. Kosterlitz and D.J. Thouless, J. Phys. C **6**, 1181 (1973); J.M. Kosterlitz, *ibid.* **7**, 1046 (1974).
 - [19] P. Olsson, Phys. Rev. Lett. **75**, 2758 (1995).
 - [20] J.V. José and G. Ramirez-Santiago, Phys. Rev. Lett. **77**, 4849 (1995); P. Olsson, *ibid.* **77**, 4850 (1995).
 - [21] E.H. Boubcheur and H.T. Diep, Phys. Rev. B **58**, 5163 (1998).
 - [22] D. Loison and P. Simon, Phys. Rev. B **61**, 6114 (2000).
 - [23] S. Faßbender, M. Enderle, K. Knorr, J.D. Noh, and H. Rieger, Phys. Rev. B **65**, 165411 (2002).
 - [24] J.V. José, L.P. Kadanoff, S. Kirkpatrick, and D.R. Nelson, Phys. Rev. B **16**, 1217 (1977).
 - [25] M. Itakura, J. Phys. Soc. Jpn. **70**, 600 (2001).
 - [26] M.S.S. Challa and D.P. Landau, Phys. Rev. B **33**, 437 (1986).
 - [27] A.M. Ferrenberg and R.H. Swendsen, Phys. Rev. Lett. **61**, 2635 (1988).
 - [28] E. Maus, Ph.D. thesis, Universität Mainz, 1991.
 - [29] K. Knorr, Phys. Rep. **214**, 113 (1992).
 - [30] K. Knorr, S. Faßbender, A. Warken, and D. Arndt, J. Low Temp. Phys. **111**, 339 (1998).
 - [31] S.W. Pierson, M. Friesen, S.M. Ammirata, J.C. Hunnicutt, and LeRoy A. Gorham, Phys. Rev. B **60**, 1309 (1999).